The Arab Journal of Scientific Research
http://aiesa.org/2017/09/the-arab-journal-of-scientific-research/

Effect of Si and EC plasticizer on the ionic conductivity enhancement of (PVA). $(NaHSO_4)_{0.5}$ solid polymer electrolyte

Sh.I. Elkalashy[2], E. Sheha[1], W. A. Ghaly[2] , M.K. El-Mansy[1]and A. I. Helal[2]

[1]*Physics Department, Faculty of Science, Benha University, Benha, Egypt*
[2] *Central Lab. for Elemental & Isotopic Analysis, NRC, AEA, Egypt*

ABSTRACT

Solid polymer electrolyte (SPE) is synthesized by solution casting technique. SPE uses poly (vinyl alcohol) PVA as a host matrix doped with solid acid $NaHSO_4$, ethylene carbonate (EC) as plasticizer and (Si) as filler. Polymer electrolytes are characterized by Impedance Spectroscopy (IS) to determine the composition of the additive which gives the highest conductivity for each system at room temperature. The ionic conductivity of the polymer electrolytes increases with temperature and obeys the Arrhenius law. X-ray diffraction (XRD) studies indicate that the conductivity increase is due to an increase in amorphous content which enhances the segmental flexibility of polymeric chains and the disordered structure of the electrolyte. Scanning electron microscopy (SEM) images show the changes morphology of solid polymer electrolyte. A magnesium battery has been fabricated with optimized composition (3.75wt. % Si) polymer electrolyte using FeS_2 as electrode which gives real capacity 112 mAh/g and has an internal resistance of 160Ω.

Keywords: Solid Polymer Electrolyte, Ethylene Carbonate**,** Si, Ionic conductivity.

1 INTRODUCTION

In order to obtain battery systems of high energy density, highly reactive components should be used, i.e. anode materials of lowest redox potential possible, and cathode materials whose redox potential is sufficiently high compared with that of anode, enabling the composition of battery systems of high working potentials. Natural candidates for anode materials for high energy density batteries are active metals such as lithium, magnesium and calcium [1]. Magnesium metal possesses a number of characteristics which make it attractive as a negative electrode material for rechargeable batteries highly negative standard potential (−2.375V versus SHE), relatively low equivalent weight (12 g per Faraday), high melting point (649 C), low cost, relative abundance, high safety, ease of handling, and low toxicity which allows for urban waste disposal [2].

Solid polymer electrolytes (SPEs) fulfill the requirements and overcome the limitations of conventional liquid electrolytes by addressing drawbacks such as electrolyte leakage, flammable organic solvent, and electrolytic degradation of electrolytes. When compared with gel polymer electrolytes (GPEs), SPEs are typically less reactive toward the electrodes. Additionally, they provide higher safety, prevent the build-up of internal pressure and can be designed in many desirable sizes and shapes. High ionic conductivity and low price are the favorable characteristics of polymer electrolyte membranes [3]. Solid acid membranes are a fascinating class of materials built upon hydrogen bonded oxyanion groups. These compounds conduct protons without the assistance of mobile water molecules, opening new technological possibilities and scientific avenues [3].

In order to enhancement electrical conductivity of polymer electrolyte at ambient temperature without affecting their stability properties to an undesirable level, various approaches are currently in vogue such as copolymerization and plasticization. The essence of plasticization is to enhance the conductivity of polymer electrolyte by means of additives of low molecular weight and high dielectric constant such as propylene carbonate (PC) ethylene carbonate (EC) and poly ethylene glycol (PEG). The addition of plasticizers could enhance the conductivity and better contact between the electrolyte\electrode [3]. The role of plasticizer should be enhancement in the fraction of amorphous phase and increasing flexibility in the polymeric segments [4]. EC has a high dielectric constant and therefore can weaken the columbic force between cation and anion and lead to ion dissociation [5].

One of the most promising ways to improve the morphological and electrochemical properties of polymer electrolytes is by the addition of ceramic fillers [6]. The addition of inorganic fillers, like glasses, alumina, silica or other ceramics, to the polymer electrolyte generally improves their transport properties, the resistance to crystallization and the stability of the electrode–electrolyte interfaces. Owing to theses merits, our current work is aimed at improving the electrical and electrochemical properties of the polymer electrolyte (PVA). $(NaHSO_4)0.5$ throught doping in different proportions of EC and Si.

2 EXPERIMENTAL METHOD

2.1 POLYMER ELECTROLYTE PREPARATION

Polymer electrolytes were prepared using solution-cast technique. Poly vinyl alcohol (PVA (C_2H_4O) n (where n = 1800) QualiKems) was used as host polymer matrix, solid acid ($NaHSO_4$) as complexation, ethylene carbonate (EC, QualiKems) as plasticizer and Si (Si, domestic source) as filler. PVA solution was prepared by adding first distilled water to the proper weight of PVA to get a 10 wt. % solution, and stirred by a magnetic stirrer at 70 °C for 6hrs. A solution of NaBr in H_2O was first added into the PVA solution under stirring at room temperature; after 2hrs H_2SO_4 was added to the solution to obtain $NaHSO_4$. After 20 min different concentrations of Ethylene Carbonate (EC), x = (0, 9.9, 13.2 and 16.5 wt. %), followed by stirring for another 2hrs. The as prepared plastizied solid acid polymer electrolyte was direct cast in a petri - glass dishes and left for month and then dried under evacuation 6 hrs at room temperature.

Si with different concentrations, Si, y = (0, 0.15, 0.75, 1.2 and 3.75 wt. %) was added to ((PVA): $(NaHSO_4)_{0.5}$ / 9.9 wt. % EC) and stirred for 12 hrs. The as prepared solution was direct cast in a perti-glass dishes and left for month at room temperature.

2.2 BATTERY PREPARATION

Generally, battery consists of two electrodes; cathode electrode was prepared by mixing, 90% FeS_2 power (source) and 10% of graphite (Qualikems) with 10 wt. % PVA solutions as a binder. The 0.5g of this mixture was compressed under pressure
2 ton, to obtain cathode pellet with an active area 1.32 cm^2 and thickness 1.51mm.

A 0.3g magnesium powder (Qualikems) was compressed under pressure2 ton to obtain anode pellet with an active area 1.32 cm^2 and thickness 1.38mm. The battery cell was then assembled by sandwiching the electrolyte between the two electrodes, anode and cathode.

2.3 CHARACTERIZATION

In order to investigate the nature of these polymer electrolyte, X-ray diffraction studies were carried out using 6000 shimazu X-ray diffractometer. The diffraction system based with Cu tube anode in the 2θ (Bragg angles) range of $0 \leq 2\theta \leq 90$ at a scan speed of 8.000(deg/min) with wave length $K_{\alpha 1}$ = 1.5418 A°. The surface morphology of the polymer electrolytes sample was observed using JEOL JSM 5600 LV SEM.

Samples of diameter 1 cm were sandwiched between the two similar brass electrodes of a spring-loaded sample holder. The whole assembly was placed in a furnace monitored by a temperature controller. The rate of heating was adjusted to be $2Kmin^{-1}$. Electrical measurements were carried out in the temperature range 303–373K using PM6304 programmable automatic RCL (Philips) meter. The measurements were carried out over a frequency range 100Hz to 100 kHz.

3 RESULT AND DISCUSSION

3.1 X-RAY DIFFRACTION INVESTIGATION

Fig.(1a.b) show XRD pattern for (((PVA): $(NaHSO_4)_{0.5}$ / x EC) where x = 0,and 9.9. A peak at 2θ=23.54° was observed in Fig. (1a), the observed peak matched quite well with JCPDS files No.85-2043 for $NaHSO_4$. This confirmed the formation of solid acid in polymer matrix. There is a relative decrease in the intensity of this peak with addition of EC. This may be due to the increase of amorphous nature of polymer electrolyte with the addition of EC. Hodge et. al. [7] established a correlation between the intensity of the peak and the degree of crystallinity. They observed that the intensity of XRD pattern decreases as the amorphous nature increases with the addition of plasticizer.

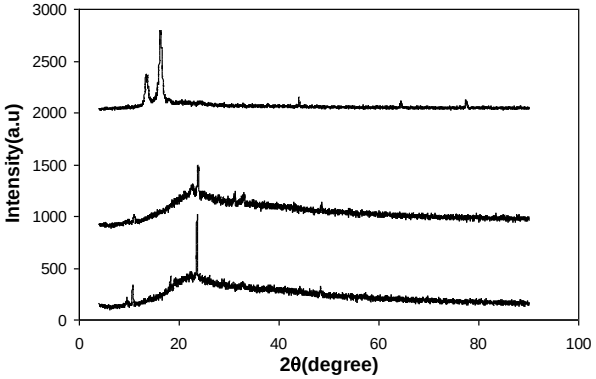

Fig.1 XRD pattern for (a) ((PVA):$(NaHSO_4)_{0.5}$), (b) ((PVA):$(NaHSO_4)_{0.5}$)/ 9.9wt.% EC), (c) ((PVA):$(NaHSO_4)_{0.5}$)/ 9.9 wt.% EC/ 3.75 wt% Si).

The structure investigation using XRD has been extended to show the influence of Si on plasticized solid acid polymer electrolyte (PSAPE). Fig. (1.c) shows XRD pattern for (((PVA): $(NaHSO_4)_{0.5}$: 9.9 wt. % EC/ 3.75 wt. % Si). There was a noticeable change in XRD peaks for samples mixed with Si in addition to the appearance of additional peaks. The results indicated that converged broad hump when the amount of Si content to (PSAPE) and appear another two peaks at 2θ =13.6, 2θ=16.6. The observed peak matched quite well with JCPDS file

No.490076 for silicon oxide sulfur (SiOS). The results suggest the occurrence of a significant new phase with the polymer electrolyte. The formation of such phase suggests that the addition of Si on the matrix cause an electrostatic interaction between Si and SO_4^{--}. This in turn leads to deduce the regality of $NaHSO_4$ lead to form more mobile H^+.

The average particle size of SAPE can be calculated using the first sphere approximation of Debye–Scherrer formula [8],

$$D = \frac{0.9\lambda}{B\cos\theta} \qquad (1)$$

where D is the average diameter of the crystals, λ is the wavelength of X-ray radiation, B is the full width at half maximum intensity of the peak and θ is the incident angle.The average particle size of $NaHSO_4$ is equal to~ 41nm. The average size of SiOS is equal to ~ 11nm.

3.2 SCANNING ELECTRON MICROSCOPE ANALYSIS

Fig. (2, a & b) shows scanning electron micrograph of ((PVA):($NaHSO_4$) $_{0.5}$/ x EC) with x = 0 and 9.9 wt. %. A comparison of the surface morphology shows marked change in the surface morphology and texture of the polymer electrolytes by the addition of EC. Surface roughening and crystalline texture of internal morphology appear to change gradually by addition of EC concentration. These effects ultimately result in the appearance of a smooth texture of the surface. Such changes can be attributed to the fact that plasticization causes a reduction in the crystallinity of the host polymer (i.e., PVA) and subsequent enhancement in the overall amorphous fraction in the material. This observation appears to be in good agreement with the XRD results.

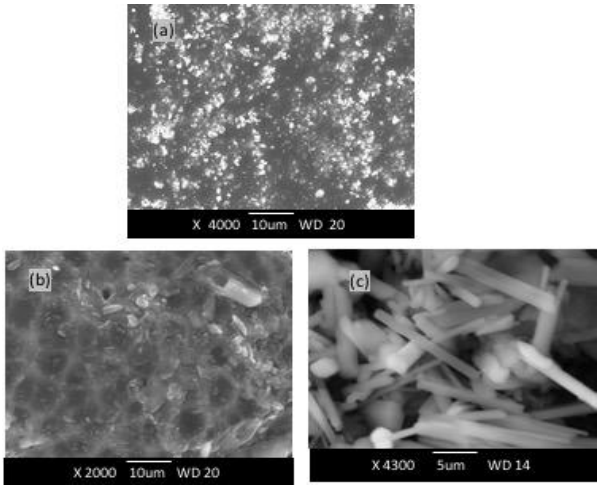

Fig.2 SEM microscope for (a) ((PVA):($NaHSO_4$) $_{0.5}$), (b) ((PVA):($NaHSO_4$) $_{0.5}$)/ 9.9wt.% EC), (c) ((PVA):($NaHSO_4$) $_{0.5}$)/ 9.9 wt.% EC/ 3.75 wt.% Si).

Fig. (2c) shows scanning electron micrograph of ((PVA): ($NaHSO_4$) $_{0.5}$: 9.9 wt. % EC/ 3.75wt. % Si). In case of Si there are long single crystals like particles having rod-shaped morphology. The sample morphology surface was uniform but with roughness indicates the formation of new phase in the host matrix.

3.3 COMPLEX IMPEDANCE ANALYSIS

The complex spectrum analysis has been carried out with an aim to observe the role of plasticizer and Si in governing the electrical properties of ((PVA): ($NaHSO_4$) $_{0.5}$). Fig.(3) shows variation of bulk conductivity for ((PVA): $NaHSO_4$) $_{0.5}$/ x EC) polymer electrolyte with x = (0, 9.9, 13.2 and 16.5 wt. %), and impedance spectrum with highest conductivity (inset) at room temperature ((PVA):($NaHSO_4$) $_{0.5}$ / 9.9wt.% EC) at 303 K.

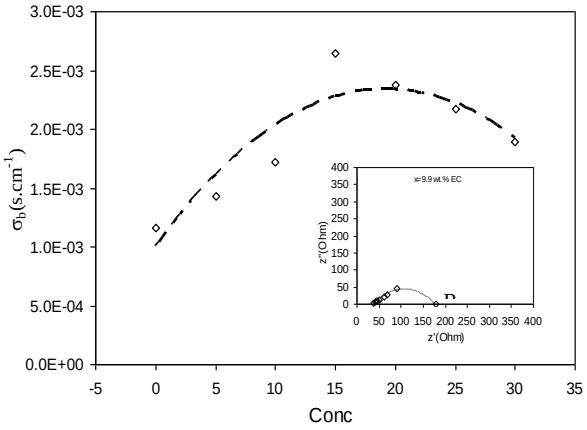

Fig.3 Variation of Bulk conductivity for ((PVA):($NaHSO_4$)$_{0.5}$)/ x EC) polymer electrolyte with different EC concentration and impedance spectrum with highest conductivity (inset) at room temperature.

It is noticed that, semicircle does not pass through the origin, and the equivalent circuit consisting of the parallel resistance (bulk resistance, R_b) and the capacitance (bulk capacitance, C_b) network in series with contact resistance [9]. Symbols Z´ and Z´´ refer to the real and imaginary components, respectively. The bulk resistance was used subsequently for evaluation the bulk conductivity,

$$\sigma_b = \frac{t}{R_b A} \qquad (2)$$

Where R_b is the bulk resistance, t is the thickness of the sample and A is the cross sectional area of the sample.

Fig.(3) illustrates the variation of bulk conductivity with EC concentration at room temperature. It can be observed that the ionic conductivity values increases with increasing plasticizer content up to 9.9 wt. % EC and then it decreases again. The variation in conductivity with EC

concentrations may be explained in terms of the number of free mobile ions. In principle, $\sigma = nq\mu$ where n is the number of free mobile ions, q is the ionic charge and μ is ionic mobility. Assuming μ to be constant σ_b increases when n increases. At the first, the increase in conductivity could be attributed to the increase in the number of free mobile ions due to dissociation of ions up to 9.9 wt. % EC. The reduction in conductivity of the electrolyte containing high amounts plasticizer (greater than 9.9 wt. % EC) could be attributed to the increase in ion pair's. Ions pairing that lead to the formation of aggregates form a more viscous medium which reduces the mobility of the charge carrier [10]. In this concentration range, the rate of ion association has to be greater than the rate of ion dissociation, and the distance between dissociated ions may become too close that it are able to recombine and form neutral ion-pairs that do not contribute towards conductivity [11].

In polymer electrolytes, there are two possible mobile ionic species, i.e., cations and anions. The type of cation expected to be responsible for the ionic conductivity in ((PVA):$(NaHSO_4)_{0.5}$ / x EC) system is H^+ ion. This H^+ ion can hop from one site to another leaving a vacancy which will be filled by another H^+ ion from a neighbouring site. Thus, the charge transport is carried out by structure diffusion or better known as Grotthus mechanism, i.e., the conduction occurs due to a dynamical effect of the anion HSO_4^- reorientation that reinforce the proton transfer in the complex[12].

Fig. (4) shows variation of bulk conductivity for ((PVA): $(NaHSO_4)_{0.5}$: 9.9 wt.% EC/ y wt.% Si) with different Si concentration y= (0.15, 0.75, 1.2& 3.75 wt.%) polymer electrolyte and impedance spectrum with highest conductivity (inset) ((PVA): $(NaHSO_4)_{0.5}$: 9.9 wt.% EC/ y wt.% Si) at 303 K.

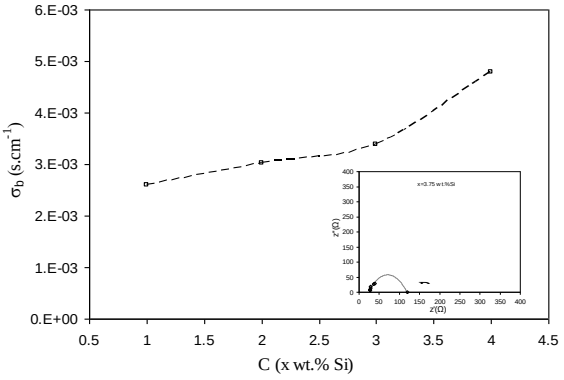

Fig.4 Variation of Bulk conductivity for((PVA):$(NaHSO_4)_{0.5}$): 9.9 wt. % EC/ y Si) with different Si concentration and impedance spectrum with highest conductivity (inset) at room temperature.

It can be observed that the bulk conductivity values increase with increasing Si concentration. As the concentration of Si increases bulk conductivity increase. The addition of Si on the matrix cause in electrostatic interaction between Si and SO_4^{--} and reduce the force between H^+ and SO_4^{--}. This in turn leads to deduce the regality of $NaHSO_4$ lead to form more mobile H^+. This causes an increase in the conductivity of the samples containing Si.

Fig.(5) show the variation of σ_{ac} with the frequency for ((PVA): $(NaHSO_4)_{0.5}$ / x EC) with x= (0, 9.9 wt.%) and ((PVA):($NaHSO_4)_{0.5}$ / 9.9 wt.% EC/ 3.75 wt.% Si). It can be observed that the conductivity increases gradually as frequency increases obeying the universal power law relation [12,13].

$$\sigma_{ac} \alpha \omega^n \qquad (3)$$

where, ω is the angular frequency and n is the power law exponent. The value of n is obtained by least square fitting equation (3) where n, are 0.2, 0.1 and 0.08 for x=0, 9.9 wt. %EC and 3.75 wt. %Si respectively. These results in the class of fast ionic conductor [12, 13].

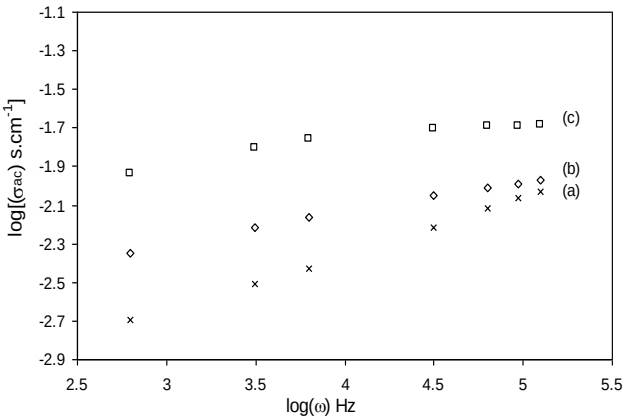

Fig.5 Variation of the ac conductivity $\sigma_{ac}(\omega)$ with frequency for (a) ((PVA):($NaHSO_4$) $_{0.5}$); (b) ((PVA):($NaHSO_4$) $_{0.5}$)/ 9.9 wt. %EC); (c) ((PVA):($NaHSO_4$) $_{0.5}$): 9.9 wt. % EC/ 3.75 wt.% Si) at room temperature.

Fig.(6) shows the variation of ac conductivity as a function of inverse temperature for ((PVA): $(NaHSO_4)_{0.5}$ / x EC) with x=(0, 9.9 wt. %) and ((PVA): $(NaHSO_4)_{0.5}$ / 9.9 wt.% EC/ 3.75 wt.% Si). The plot shows that as temperature increases, the conductivity increases. Regression values are close to (0.91-0.99) suggesting that all the points lie on a straight line.

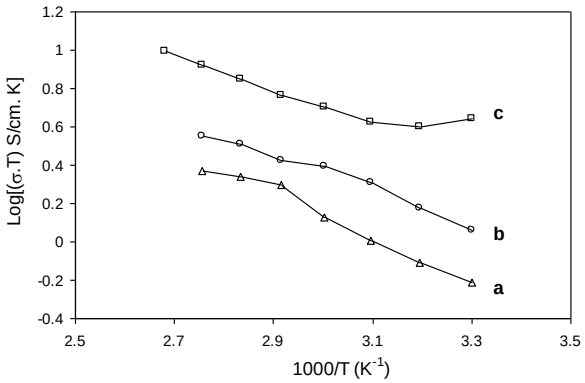

Fig.6 Arrhenius plot of the ionic conductivity for (a) ((PVA):($NaHSO_4$) $_{0.5}$); (b) ((PVA):($NaHSO_4$) $_{0.5}$)/ 9.9 wt. %EC); (c) ((PVA):($NaHSO_4$) $_{0.5}$): 9.9 wt. % EC/3.75wt.% Si).

The conductivity values for the PSAPE do not show any abrupt jump with temperature indicating that these electrolytes exhibit a completely amorphous nature that facilitates the fast ion motion in the polymer net work and it further provides a higher free volume in the polymer electrolyte upon increase in temperature. The temperature dependence of conductivity can be described by [14],

$$\sigma_{ac}.T = B\exp(\frac{-E_a}{KT}) \qquad (4)$$

where B is the temperature independent constant , E_a is activation energy, K is Boltzman constant and T is absolute temperature. The activation energies for ion migration calculated from the slope of the log σT vs.10^3/T plots, it is clear, the E_a values are 0.26, 0.16 and 0.18 eV for x= 0, 9.9 wt. %EC and 3.75 wt. %Si respectively. It is noteworthy that the polymer electrolytes with low values of activation energies are desirable for practical applications. There is a significant conductivity enhancement due to the addition of the plasticizer, EC to SAPE. Also, the presence of (Si) has shown a conductivity enhancement of the PSAPE. The highest room temperature conductivity enhancement was obtained for ((PVA): ($NaHSO_4$) $_{0.5}$: 9.9 wt. % EC/3.75wy.% Si) was 1×10^{-2} S.cm^{-1} (at 303 K).

3.4 TRANSFERENCE NUMBER MEASUREMENT

Transference number is an important parameter in studying type of conduction in solid polymer electrolyte. The transference numbers, both ionic (t_{ion}) and electronic (t_{ele}), of the electrolyte were evaluated using the Wagner's polarization techniques. The dc current was monitored as a function of time on application of fixed dc voltages 1.5volt across Cu / ((PVA: ($NaHSO_4$) $_{0.5}$ / x EC)/ Cu with x=0, 9.9 wt. %. Fig.(7a.b) and Cu / ((PVA):($NaHSO_4$) $_{0.5}$ / 9.9wt.% EC: 3.75wt.%Si)/ Cu Fig.(7c) illustrate current versus time plot for the electrolyte.

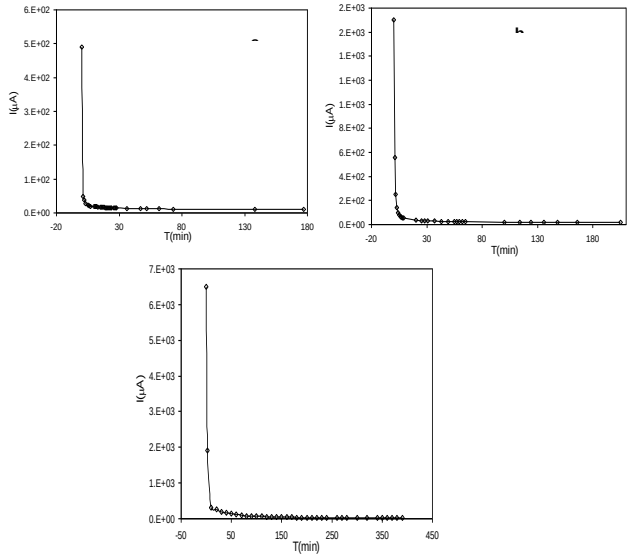

Fig.7 Polarization current as a function of time for (a) ((PVA):($NaHSO_4$) $_{0.5}$); (b) ((PVA):($NaHSO_4$) $_{0.5}$)/ 9.9 wt. %EC); (c) ((PVA):($NaHSO_4$) $_{0.5}$): 9.9 wt. % EC/3.75wt.% Si).

The initial current is due to the total current (i_t) which is due to the ionic (i_{ion}) and the electronic (i_{ele}). As the polarization build up the i_{ion} is blocked and the final current is only the electronic current [14,15].

$$i_\tau = i_{ele} + i_{ion} \qquad (5)$$

And

$$t_{ion} = \frac{i_\tau - i_{ele}}{i_\tau} \qquad (6)$$

$$t_{ele} = \frac{i_{ele}}{i_\tau} \qquad (7)$$

The transference number has been extracted, the electron fraction is t_{ele}=0.01 and ion fraction is t_{ion}=0.99 for x=9.9 wt. % EC and 3.75wt. %Si the blank sample(x=0 wt. % EC) the electron fraction is (t_{ele}) =0.03 and ion fraction is (t_{ion}) =0.97 so, current is predominantly due to ions with negligible contribution coming from the electrons.

3.5 BATTERY CHARACTERIZATION

Fig.(8) Shows the discharge characteristic of the battery Mg / ((PVA): ($NaHSO_4$) $_{0.5}$ / 9.9 wt. % EC: y wt. % Si) / FeS_2 at constant load, R=50 kΩ. The discharge voltage

was sustained for 67.5h until the cut-off voltage of 0.51*V*. The extracted value of cell capacity for Mg / ((PVA): $(NaHSO_4)_{0.5}$: 9.9 wt. % EC/ y wt. % Si)/ FeS_2 was 1.12 mAh which evaluated from equation [16],

$$C = \frac{1}{R}\int_0^t V(t)dt \qquad (8)$$

Estimated capacitance is only for surface area of electrode. Since the electrodes used in this cell is in compact planar form, this mean that electrodes are not fully utilized for discharge reaction.

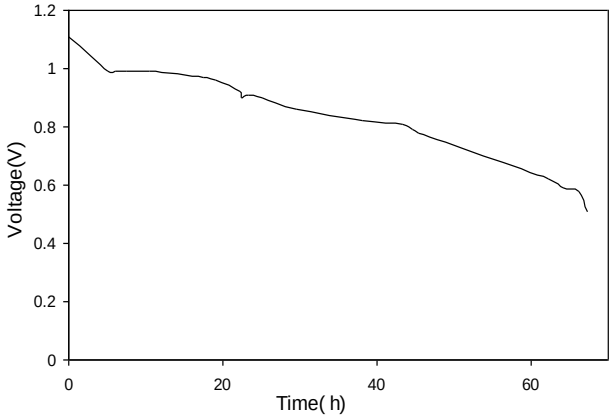

Fig.8 Discharge plot for Mg/((PVA):$(NaHSO_4)_{0.5}$): 9.9 wt.% EC: 3.75 wt.% Si)/ FeS_2 cell at constant load of 50 kΩ.

The active weight of Mg was deduced by < 0.01 gm. Therefore, the real discharge capacity can be estimated by >112mAh/gm for Mg / FeS_2. After Mg / FeS_2were fully discharged, a layer of white powder was formed. The *XRD* confirmed that the white powder is $MgSO_4$. Based on the *XRD* data, the failure of the anode is due to the sulfation of Mg which formed $MgSO_4$. Sulfation [17] is the number one cause of the battery failure. It is identified empirically by observing the effects of: Loss of capacity, Loss of voltage and increase in internal resistance.

Fig.(9 a & b) shows the comparative XRD patterns of virgin Mg and Mg after discharge. The XRD pattern indicated that some characterist peak disappeared where as new peak appeared after discharge, the observed peaks matched quite well with JCPDS file No. 72-1068 for $MgSO_4$ at 2θ= 15, 34.6 and 36.9. Thus, it is confirmed that the structure is indeed $MgSO_4$.

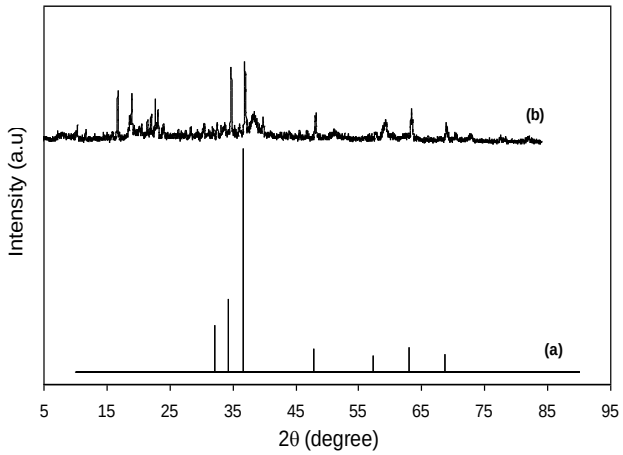

Fig.9 XRD patterns of Mg electrode (a) Virgin Mg, (b) Mg after complete discharge at 50 kΩ.

Fig.(10a & b) shows the comparative XRD patterns of the vergin FeS_2 cathode and after the discharge, respectively. After discharge the *XRD* pattern indicated that FeS_2 deos not change, the characterist peak also not change but intensity of the peak decrease.The drop of the intensity of the peakcan be attribute to the strain experine due to the interculation of the ion with Fes_2 during discharge.

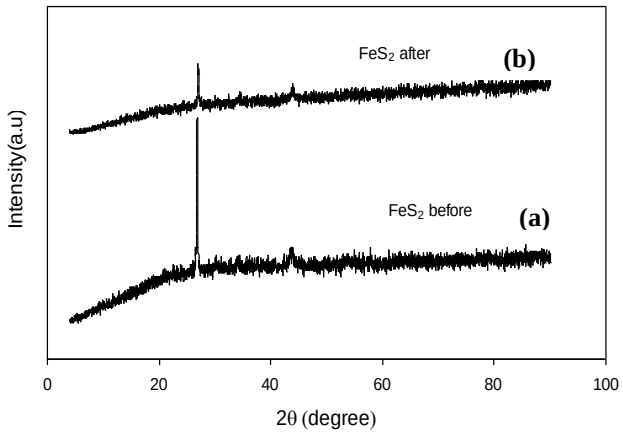

Fig.10 XRD patterns of FeS_2 electrode (a) Virgin FeS_2, (b) FeS_2 after complete discharge at 50 kΩ.

Fig.(11) shows the *I-V* and *J-P* characteristics for Mg /((PVA): $(NaHSO_4)_{0.5}$: 9.9wt. % EC/ 3.75wt. % Si) / FeS_2 battery at room temperature.

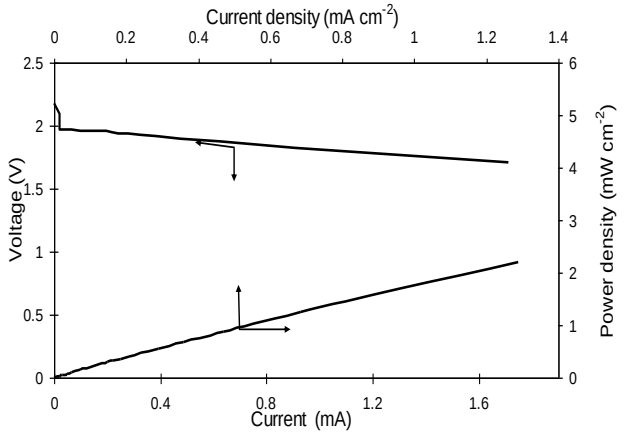

Fig.11 I-V and J-P curves for Mg/((PVA):($NaHSO_4$) $_{0.5}$): 9.9 wt.% EC / 3.75 wt.% Si) /FeS_2 cell.

I-V curve had a simple linear form which indicates that polarization on the electrode was primarily dominated by ohmic contributions. The internal resistance of the Mg / FeS_2 battery was obtained from the gradient of the *I-V* graph, which was 160Ω. The voltage of the Mg / FeS_2 battery dropped to a short circuit density of 1.3mA/cm^2 and maximum power density 2.2 mW/cm.

4 CONCLUSIONS

From the obtained results and discussions one can conclude the following:

1. We succeed to develop polymer electrolyte based on Poly (vinyl alcohol) (PVA) complexed with ($NaHSO_4$) and ethylene carbonate (EC) as plasticizer ((PVA):($NaHSO_4$) $_{0.5}$ / x wt.% EC) and add Si to the electrolyte.
2. XRD for polymer electrolyte show the addition of EC reduce the degree of crystalline of $NaHSO_4$ where the addition of Si occurrence of a significant new structure.
3. We succeed to increase bulk conductivity σ_b reached from 4.5 $\times 10^{-3}$ S.cm^{-1} with 9.9 wt. % EC to 1 $\times 10^{-2}$ S.cm^{-1} with 3.75 wt. % Si in the present polymer electrolyte.
4. The transference number data in these polymer electrolytes have shown that the conduction is predominantly due to ions.
5. A magnesium battery has been successfully fabricated with optimized composition (3.75wt. % Si) using FeS_2 as electrode which gives real capacity 112 mAh/g and has an internal resistance of 160Ω.

5 REFERENCES

[1] Aurbach D, Gofer Y, Z.Lu, schechter A , chusid O, H. Gizbar, Cohen Y, Ashkenazi V, Turgeman R , Levi E. A short review on the comparion between Li battery systems and rechargeable magnesium battery technology. J. power sources 2001 ;(97-98): 28-32.

[2] Sun Oh Ji, Myoun Ko Jang, Won Kim Dong. Preparation and characterization of gel polymer electrolytes for solid state magnesium batteries. J.Electrochimica Acta. Acta 2004 ; 50 (903–906):

[3] Sheha E. Prepartion and physical properties of (PVA) 0.75 (NH4Br)0.25(H2SO4)xM solid acid membrane J. Non-Crystalline Solids 2010; 356: 2282-2285.

[4] Mohamad A A and Arof A K. Plasticized alkaline solid polymer electrolyte system. J. Material Letters 2007; 61: 3096-3099.

[5] Ratner M A, Polymer Electrolyte Reviews1, J.R. Maccallum and C.A.Vincent, p.173, Elsevier Appl. Science, London 1987.

[6] Krawiec W, Jr Scanlon L G, Fellner j p , Vaia R A , Vasudevan S , Giannelis E P. Polymer nanocomposites: a new strategy for synthesizing solid electrolytes for rechargeable lithium batteriesPolymer nanocomposites: a new strategy for synthesizing solid electrolytes for rechargeable lithium batteries J. Power Sources 1995 ; 54: 310-315.

[7] Hodge M R, Edward, Graham H, Simon G P, Water absorption and states of water in sernicrystalline poly(vinyl alcohol) films J. Polymer 1996; 37: 1371-1376.

[8] Pejova B and Grozdanov I ,Three-dimensional confinement effects in semiconducting zinc selenide quantum dots deposited in thin-film form J. Material Chemistry and Physics 2005 ; 90: 35-46.

[9] Suman C K, Yun J, Kim S, Lee Sin-Doo, Lee Changee, AC impedance spectroscopic studies of transport properties in metal oxide doped α-NPD J. Current applied Physics. 2009; 9: 978-984.

[10] Subban R H Y, Arof A K Plasticiser interactions with polymer and salt in PVC–LiCF3SO3–DMF electrolytes J. European polymer 2004;40: 1841-1847.

[11] Majid S R, Arof A K, FTIR Studies of Chitosan-Orthophosphoric Acid-Ammonium Nitrate-Aluminosilicate Polymer Electrolyte J. Molecular. Crystal. Liquid Crystal 2008; 484: 117-126.

[12] Sheha E. Ionic conductivity and dielectric properties of plasticized PVA0.7(LiBr)0.3(H2SO4)2.7M solid acid membrane and its performance in a magnesium

battery J. Solid State Ionics 2009 ;180: 1575-1579.

[13] Sheha E, El-Mansy M K. A high voltage magnesium battery based on H2SO4-doped (PVA)0.7(NaBr)0.3 solid polymer electrolyte J. power sources 2008;185: 1509-1513.

[14] Awadhia A, Patel S K, Agrawa S L. Dielectric investigations in PVA based gel electrolytesJ. Progress in Crystal Growth and Characterization of Materials . 2006; 52: 61-68.

[15] Ramesh S, Yahaya A H, Arof A K. Dielectric behaviour of PVC-based polymer electrolytes J. Solid State Ionics 2002; 152-153: 291-294.

[16] Cui N, Luo J L. Effects of oxide additions on electrochemical hydriding and dehydriding behavior of Mg2Ni-type hydrogen storage alloy electrode in 6 M KOH solution J. Electrochimica Acta 1998; 44: 711-720.

[17] Catherino A H, Feres F F, Trinidad F. Sulfation in lead–acid batteries J. Power Sources 2004; 129: 113-120.